Supplementary Materials

Adsorption of Lead from Water Using MnO_2-Modified Red Mud: Performance, Mechanism, and Environmental Risk

Yang Bai [1,2], Yin Pang [2], Zheng Wu [2], Xi Li [1], Jiang Jing [1], Hongbin Wang [3] and Zheng Zhou [1,*]

[1] School of Materials and Environmental Engineering, Chengdu Technological University, Chengdu 611730, China
[2] Faculty of Geosciences and Environmental Engineering, Southwest Jiaotong University, Chengdu 611756, China
[3] Sichuan Provincial Engineering Research Center of City Solid Waste Energy and Building Materials Conversion and Utilization Technology,
Chengdu 610106, China
* Correspondence: lswtqzz@163.com

Text S1 Chemicals and materials

The original red mud was obtained from an aluminum plant in Chongqing (Chongqing Municipality, China), where industrial alumina refining is the combined process. The main chemical composition of red mud included: CaO (30.32 %), SiO_2 (21.42 %), Fe_2O_3 (14.90 %), Al_2O_3 (10.96 %), Na_2O (7.03 %), TiO_2 (5.60 %), MgO (0.58 %), K_2O (0.26 %), with a burn vector of 6.4 %.The raw materials were crushed and passed through a 100 mesh sieve. The sample was dried in an oven (DHG-9240A, Shenzhen) at 105°C for 48 h, sealed and stored in plastic bags as experimental raw materials, and named RM.

Potassium permanganate ($KMnO_4$), manganese sulfate monohydrate ($MnSO_4 \cdot H_2O$), cadmium nitrate tetrahydrate ($Cd(NO_3)_2 \cdot 4H_2O$), nitric acid (HNO_3), sodium hydroxide (NaOH), calcium chloride ($CaCl_2$), magnesium chloride ($MgCl_2$), potassium chloride (KCl) and sodium chloride (NaCl), are analytically pure and used without further purification. The water used for the experiments was deionized water.

Text S2 Characterization methods for Mn-RM

In this study, the crystal phase and composition of the sample was analyzed by the X-ray diffractometer (XRD, RIGAKU, Japan), with the conditions of Cu Kα as the radiation, λ=1.5406 Å, and scanning speed of $5°\cdot min^{-1}$. The scanning electron microscope (SEM) and energy-dispersive spectroscopic (EDS, JSM-7500F, Japan) were obtained to investigate surface morphology and elemental composition changes of the samples. The specific surface area of the samples was measured by N_2 adsorption-desorption experiments at 200℃ with a degassing time of 6h using a Mike 2460 physisorption instrument and calculated by the Brunauer-Emmett-Teller (BET). The pore size of the sample was measured and calculated by Barret-Joyner-Halender (BJH) method in the N_2 adsorption-desorption experiments. Fourier transform infrared spectrometer (FTIR, Nicolet 670, USA) was used to measure the infrared spectra of the samples and analyze the functional groups contained in the samples. In addition, the samples' X-ray photoelectron spectroscopy (XPS, Thermo Scientific K-Alpha, USA) was made with Al Kα (hv=1486.6eV) rays as the excitation source corrected for C1s=284.80eV binding energy to investigate the adsorption mechanism further.

Text S3 Details of batch experiments

(1) Adsorption kinetics

A conical flask with 100 mL solution including Pb^{2+} (initial concentration = 500 $mg \cdot L^{-1}$) and 1.0 g L^{-1} of Mn-RM. The initial pH of solution was adjusted to 5.0 by using 1.0 M NaOH or 1.0 M HNO_3, and the supernatant was achieved at 10, 20, 30, 60, 90, 120, 150, 180, 240, 300, 360, 420, and 480 min after through a 0.45μm filter membrane, and then the residual concentration of Pb^{2+} was determined by atomic absorption spectrophotometry (Hitachi Z-2000, Japan). All the experiments were carried out on a shaker and the speed was set at 200 rpm at 25 ℃ and prepared in triplicate. Experimental data of kinetics were fitted by four classical models: the pseudo-first-order (Eq.(1)), the pseudo-second-order (Eq.(2)), the Elovich model (Eq.(3)) and Intra-particle diffusion (Eq.(4)) [1].

$$Q_t = Q_e(1-e^{-k_1 t}) \tag{1}$$

$$Q_t = \frac{k_2 Q_e^{\,2}}{1+k_2 Q_e t} \tag{2}$$

$$Q_t = \ln(\alpha\beta)/\beta + \ln t/\beta \tag{3}$$

$$Q_t = k_i' t^{0.5} + C_i \tag{4}$$

Where Q_e ($mg \cdot g^{-1}$) and Q_t ($mg \cdot g^{-1}$) are the adsorption amount towards Pb^{2+} at equilibrium and at time t, respectively. k_1(min^{-1}), k_2 ($g \cdot (mg \cdot min)^{-1}$), α ($mg \cdot (g \cdot min)^{-1}$), β ($g \cdot mg^{-1}$) and k_i' (mg $(g \cdot min^{0.5})^{-1}$) are the rate constants of diverse kinetics(Eq.(1)~Eq.(4)); C_i is to describe the boundary layer characteristic.

(2) Adsorption isotherms and thermodynamics

The concentrations of Pb^{2+} were set at 0, 100, 200, 300, 400, 500, 600, and 700

mg·L^{-1}, respectively, and with 1.0 g L^{-1} Mn-RM. The conical flasks containing Pb^{2+} and biochar were carried out on a shaker (200 rpm) for 240min. The initial pH of solution was adjusted to 5.0 by using 1.0 M NaOH or 1.0 M HNO_3. The Langmuir (Eq. (5)), Freundlich (Eq. (6)) and Sips (Eq. (7)) isotherm model were applied in this study.

$$\mathrm{Q_e} = \frac{Q_0 K_L C_e}{1 + K_L C_e} \tag{5}$$

$$\mathrm{Q}_e = K_F C_e^{1/n} \tag{6}$$

$$\mathrm{Q}_e = \frac{Q_0 (\mathrm{K}_S C_e)^{1/m}}{1 + (K_s C_e)^{1/m}} \tag{7}$$

Where Q_e (mg·g^{-1}) and Q_0 (mg·g^{-1}) are the equilibrium and the maximum adsorption capacity, respectively; C_e (mg·L^{-1}) represents the equilibrium concentration of Pb^{2+}; K_L (L·mg^{-1}), K_F and K_S (L·mg^{-1}) represent the constants of Langmuir, Freundlich and Sips, respectively. *n* and *m* are the empirical parameters of Freundlich and Sips, respectively.

Thermodynamic studies were conducted to determine whether the adsorption of Pb^{2+} by Mn-RM is exothermic or endothermic. The impact of temperature on the adsorption performance of Mn-RM for Pb^{2+} was investigated at three different temperatures: 25°C, 45°C, and 65°C. To obtain key thermodynamic parameters, such as the standard Gibbs free energy change (ΔG, kJ/mol), standard enthalpy change (ΔH, kJ/mol), and standard entropy change (ΔS, J/mol•K), the plot of ln(K_C) against 1/T was further analyzed using Eq. (8-10) [2].

$$\Delta \mathrm{G} = -\mathrm{RT} \ln\left(K_C\right) \tag{8}$$

$$K_C = \frac{C_e(\text{ adsorbent })}{C_e(\text{ solution })} \tag{9}$$

$$\ln\left(K_C\right)=\frac{\Delta S}{R}-\frac{\Delta H}{RT} \tag{10}$$

where R is the gas constant (8.314 J/mol•K), T is the temperature (K), K_C is the equilibrium constant, and C_e (*adsorbent*) and C_e (*solution*) are the Pb^{2+} concentrations (mg/L) on the adsorbent and in solution at equilibrium (mg/L), respectively.

(3) Multi-factors effect on adsorption experiment

In order to research the effect of multi-factors on the removal efficiency of Pb^{2+}, three independent variables (initial pH, solid-liquid ratio (w/v) and initial concentration of Pb^{2+}) were chosen. The pH of liquid was adjusted by using 1.0 M NaOH or 1.0 M HNO_3. And the solid-liquid ratio was adjusted with adding different volumes of distilled water. All experiments were designed by Design Expert 10 software.

(4) Effect of co-cation types on Pb^{2+} adsorption

100 mL solution of Pb^{2+} (500 mg·L^{-1}) and Mn-RM (0.1 g) were placed in a conical flask, The pH of liquid was adjusted to 5.0 by using 1.0 M NaOH or 1.0 M HNO_3. The solution contained a kind of cation with four concentrations, containing Na^+, K^+, Mg^{2+}, and Ca^{2+}, which the concentrations were all 40 mg·L^{-1}.

(5) Adsorption-regeneration experiments

The regeneration ability as a very crucial index for Mn-RM was researched in this study. The regeneration treatments is EtOH and 80℃ water bath. Specifically, after each adsorption round, Mn-RM was regenerated, and then washed by deionized water until the elute was nearly neutral. The regeneration efficiency of Mn-RM was calculated according to Eq. (11) by using EtOH to regenerate.

$$\text{Regeneration efficiency (\%)} = \frac{C_t V}{m Q_e} \times 100\% \quad (11)$$

Where Q_e (mg·g^{-1}) and C_t (mg·L^{-1}) are the equilibrium adsorption capacity and the concentration of Pb^{2+} after regeneration, respectively. m (g) and V (L) are the mass of Mn-RM and the volume of solution.

Text S4 **Methods and Procedures of environmental risk assessment**

In order to obtain insights into the environmental toxicity of Mn-RM under different leaching scenarios, which is related to the the content and chemical speciation of heavy metals (HMs) [3,4]. Thus, the risk assessment code (RAC) model and synthesis toxicity index (STI) model were adopted respectively for environmental risk assessment of HMs in Mn-RM.

RAC model can assess the independent toxicity of each HM according to their proportion of bioavailable fractions (T1 and T2) [5,6]. The values of RAC were calculated by using Eq. (12). The environmental risk of each HM can be classified into five levels (Li et al., 2019; Pan et al., 2013): safe (RAC ≤ 1%), low risk (1% < RAC ≤ 10%), medium risk (10% < RAC ≤ 30%), high risk (30%< RAC ≤50%), very high risk (RAC > 50%).

$$\mathrm{RAC} = \frac{\mathrm{T1+T2}}{\mathrm{T1+T2+T3+T4+T5}} \times 100\% \tag{12}$$

Where T1 (exchangeable), T2 (carbonate-bound), T3 (Fe/Mn oxide-bound), T4 (organic-bound), and T5 (residual) are the five chemical speciation fractions of each HM, respectively.

STI model considered the type, number, chemical speciation, toxicity, stability, and background value of targeted HMs simultaneously [7]. The values of STI were calculated by using Eq. (13).

$$\mathrm{STI} = \sum_{i=1}^{n} \left[\frac{T_i \times (\sum_{j=1}^{m} (E_j \times Q_i^j))}{C_n^i} \right] \tag{13}$$

Where i is the type of targeted HMs; n is the number of HMs (n=6); j is the type

of chemical speciation of each HM (T1, T2, T3, T4, and T5); m is the number of chemical speciation of each HM (m=5); T_i is the toxicity coefficient of the i-th HM (Table S6), which is used to characterize the environmental toxicity of HMs [7]; E_j is the bioavailability coefficient of the j-th chemical speciation of each HM (Table S6); is the mass concentration of the j-th chemical speciation of the i-th HM (mg/kg); C_n^i is the background value of the i-th HM (mg/kg).

Table S1 **Box-Behnken Design for Pb^{2+} adsorption by Mn-RM.**

number	Design						Actual (Y_1)	Predicted (Y_1)
	Codes			Factors				
	A	B	C	pH	Solid-liquid ratio ($g \cdot L^{-1}$)	Initial Pb^{2+}concentration ($mg \cdot L^{-1}$)	Removal efficiency of Pb^{2+} (%)	Removal efficiency of Pb^{2+} (%)
1	-1	-1	0	4	0.6	450	58.21	66.28
2	1	-1	0	6	0.6	450	81.51	74.24
3	-1	1	0	4	1	450	71.48	67.16
4	1	1	0	6	1	450	83.20	86.72
5	-1	0	-1	4	0.8	300	75.92	73.91
6	1	0	-1	6	0.8	300	88.75	90.49
7	-1	0	1	4	0.8	600	65.57	63.83
8	1	0	1	6	0.8	600	72.75	74.77
9	0	-1	-1	5	0.6	300	84.78	84.51
10	0	1	-1	5	1	300	59.07	59.61
11	0	-1	1	5	0.6	600	40.57	40.03
12	0	1	1	5	1	600	78.03	78.29
13	0	0	0	5	0.8	450	93.61	95.2
14	0	0	0	5	0.8	450	96.80	95.2
15	0	0	0	5	0.8	450	95.37	95.2
16	0	0	0	5	0.8	450	94.02	95.2
17	0	0	0	5	0.8	450	96.19	95.2

Table S2 **BET surface area, pore volume and average pore diameter of the RM and MRM.**

Sample	RM	Mn-RM
specific surface area（$m^2 \cdot g^{-1}$）	10.2212	82.4536
Pore volume（$cm^3 \cdot g^{-1}$）	0.018292	0.148757
Average pore diameter（nm）	22.1247	7.2165

Table S3 **Adsorption thermodynamic parameters for Mn-RM on Pb^{2+}**

	Initial concentration ($mg \cdot L^{-1}$)	ΔH ($kJ \cdot mol^{-1}$)	ΔS ($J \cdot mol^{-1} \cdot K^{-1}$)	ΔG($kJ \cdot mol^{-1}$)		
				25℃	45℃	65℃
Pb^{2+}	100	1.85	25.15	-2.04	-2.23	-2.42
	200	2.27	26.19	-2.00	-2.17	-2.39
	300	2.87	27.58	-1.90	-2.14	-2.33

Table S4 ANOVA for response surface quadratic model.

Source	Sum of squares	df[a]	Mean square	F value[b]	P-value(Prob > F)[c]
Model	4024.68	9	447.19	84.37	< 0.0001
A	378.29	1	378.29	71.37	< 0.0001
B	89.16	1	89.16	16.82	0.0046
C	332.76	1	332.76	62.78	<0.0001
AB	33.56	1	33.56	6.33	0.0400
AC	7.97	1	7.97	1.50	0.2598
BC	997.87	1	997.87	188.26	< 0.0001
A^2	138.28	1	138.28	26.09	0.0014
B^2	1060.17	1	1060.17	200.02	< 0.0001
C^2	792.66	1	792.66	149.55	< 0.0001
Residual	37.10	7	5.30		
Lack of Fit	29.59	3	9.86	5.25	0.0714
Pure Error	7.51	4	1.88		
Cor Total	4061.79	16			

[a] Degree of freedom.

[b] Test for comparing model with residual (error) variance.

[c] Probability of finding the observed F value when the null hypothesis is true.

[s] Significant at $P < 0.05$.

[e] Not significant at $P > 0.05$.

Table S5 Validation of RSM results.

	Pb^{2+} removal efficiency
Prediction	87.45
Experiment 1	87.01
Experiment 2	87.26
Experiment 3	87.34
Mean	87.20
Relative error	0.028%

Table S6 **Bioavailability coefficient of each chemical speciation of HMs.**

Chemical Speciation	Exchangeable	Carbonate-bound	Fe/Mn oxide-bound	Organic-bound	Residual
E_j	7	5	5	2	0

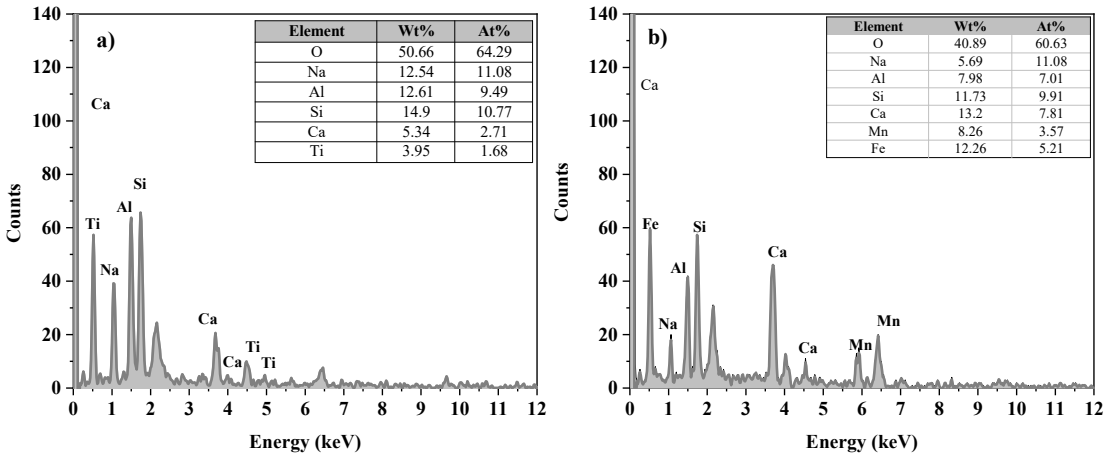

Fig. S1. EDS mapping of (a) RM and (b) Mn-RM.

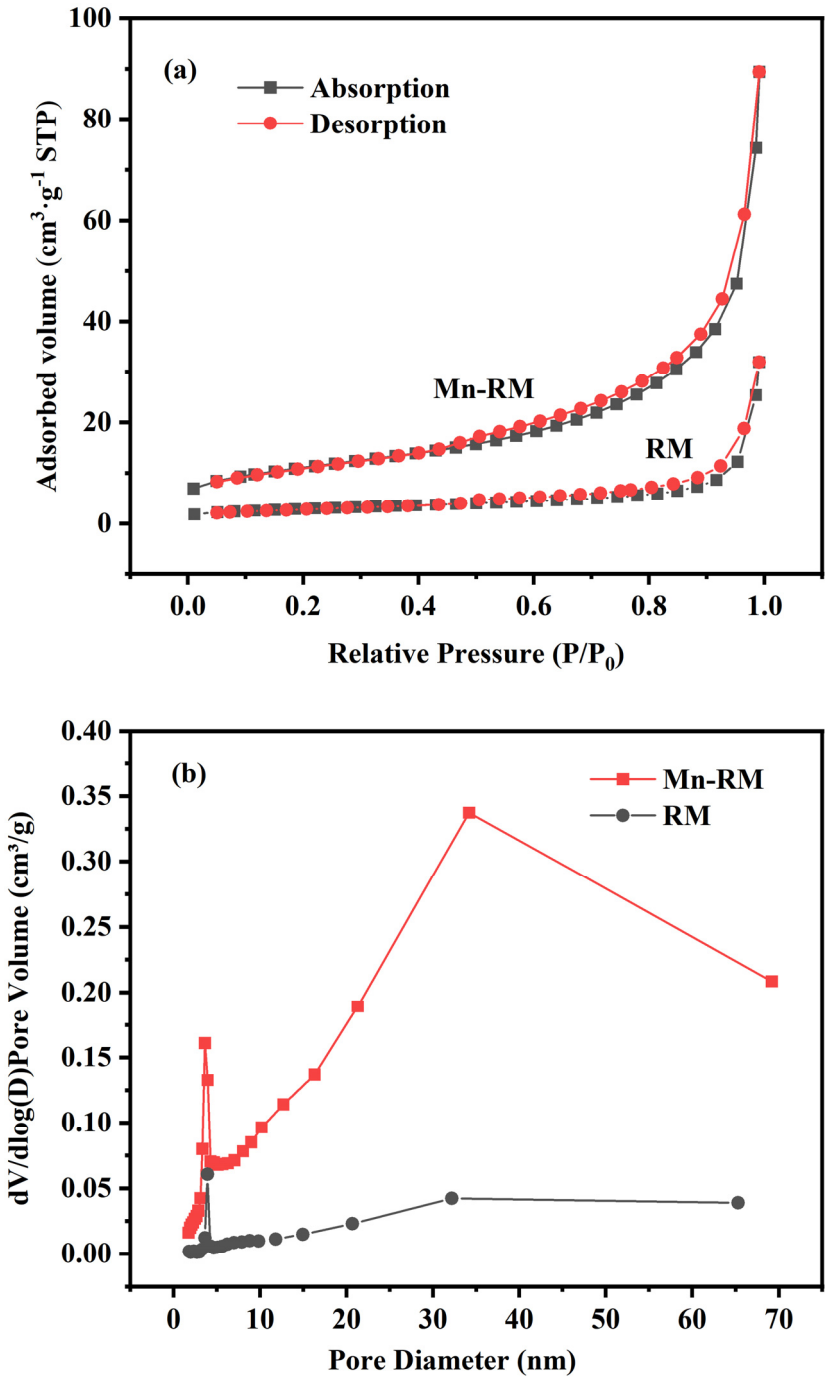

Fig. S2. (a) N_2 Adsorption-Desorption Isotherms and (b) Pore Size Distribution of RM and Mn-RM.

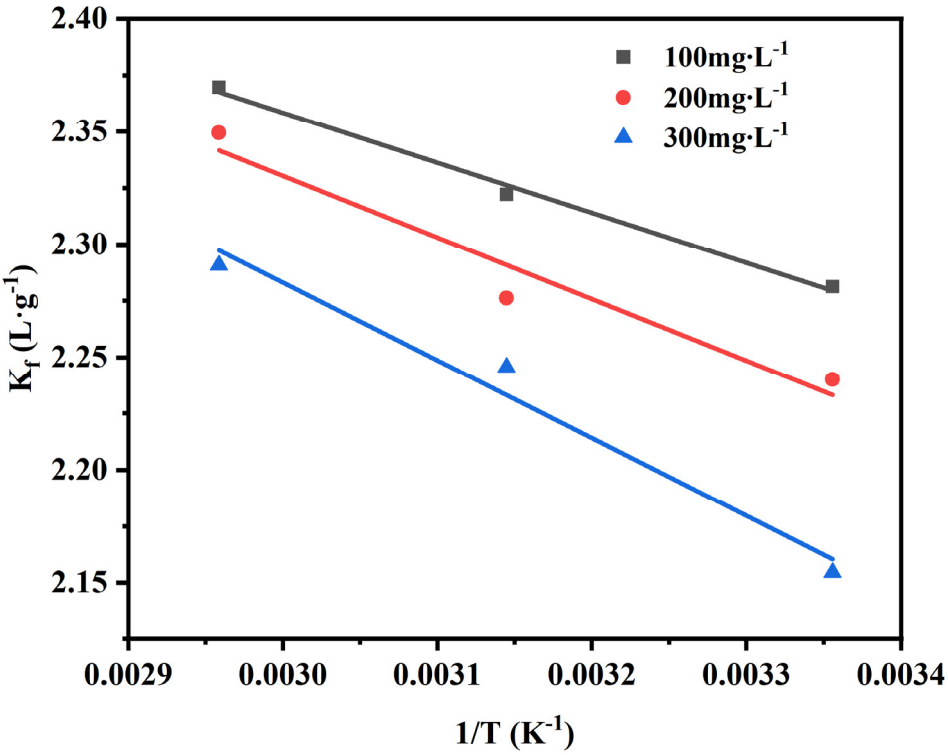

Fig. S3. Thermodynamic Curves of Mn-RM for Pb^{2+} adsorption.

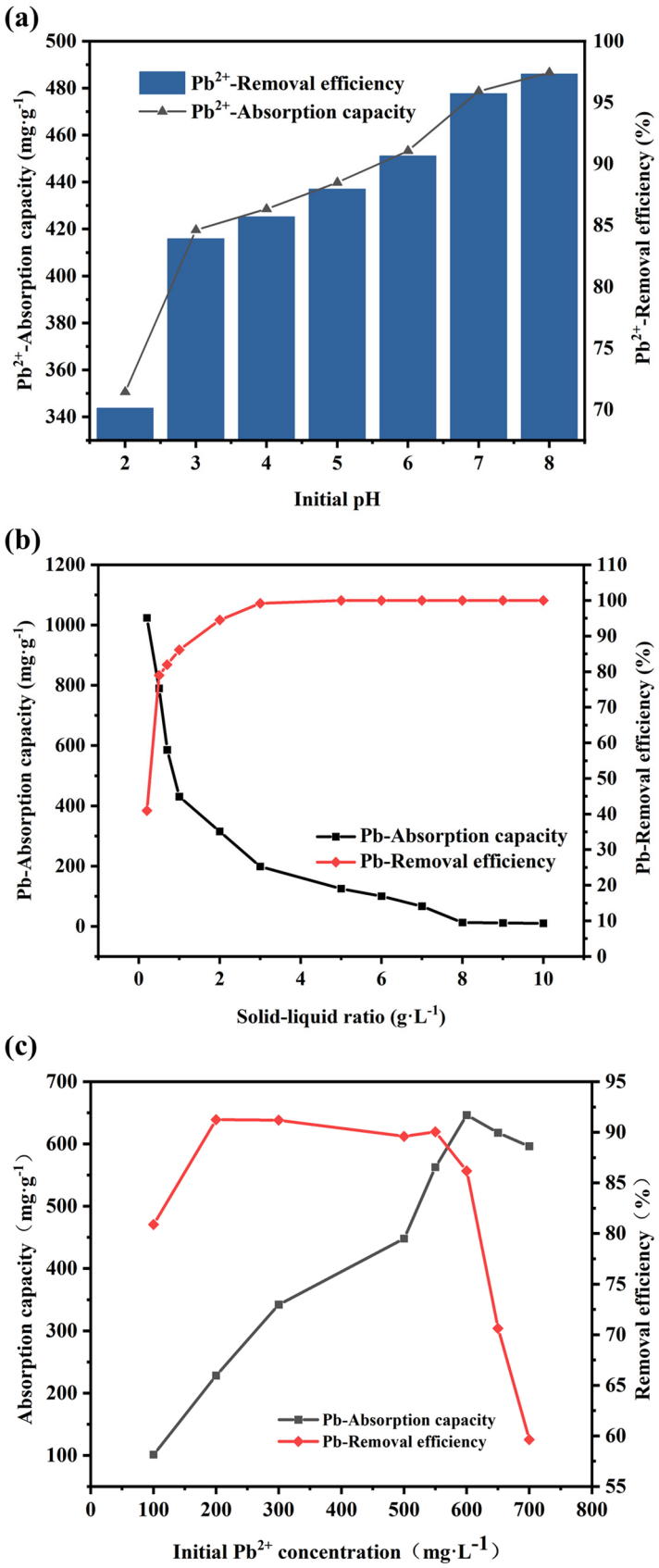

Fig. S4. Effects of (a) initial pH, (b) solid-liquid ratio (w/v) and (c) initial Pb^{2+} concentration on Pb^{2+} adsorption by Mn-RM.

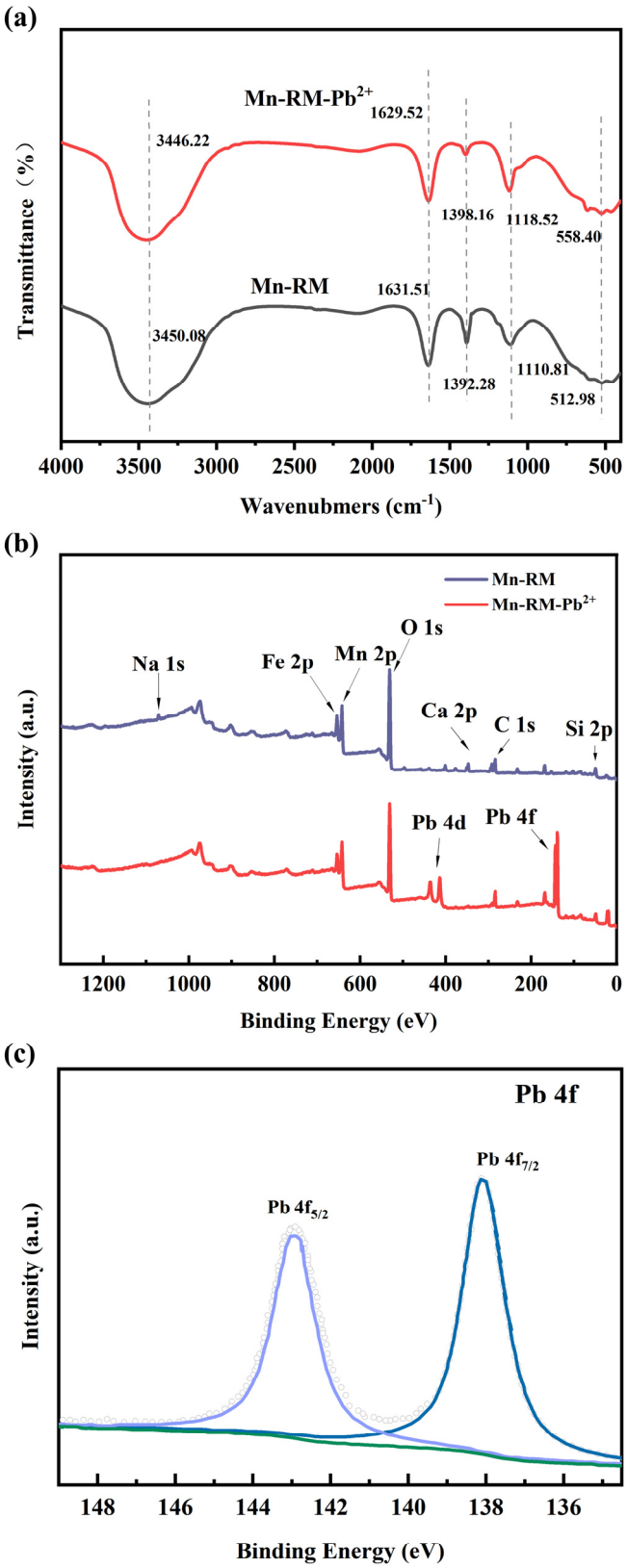

Fig. S5. (a) FTIR, (b) XPS survey, and (c) Pb 4f spectra of Mn-RM after Pb^{2+} adsorption.

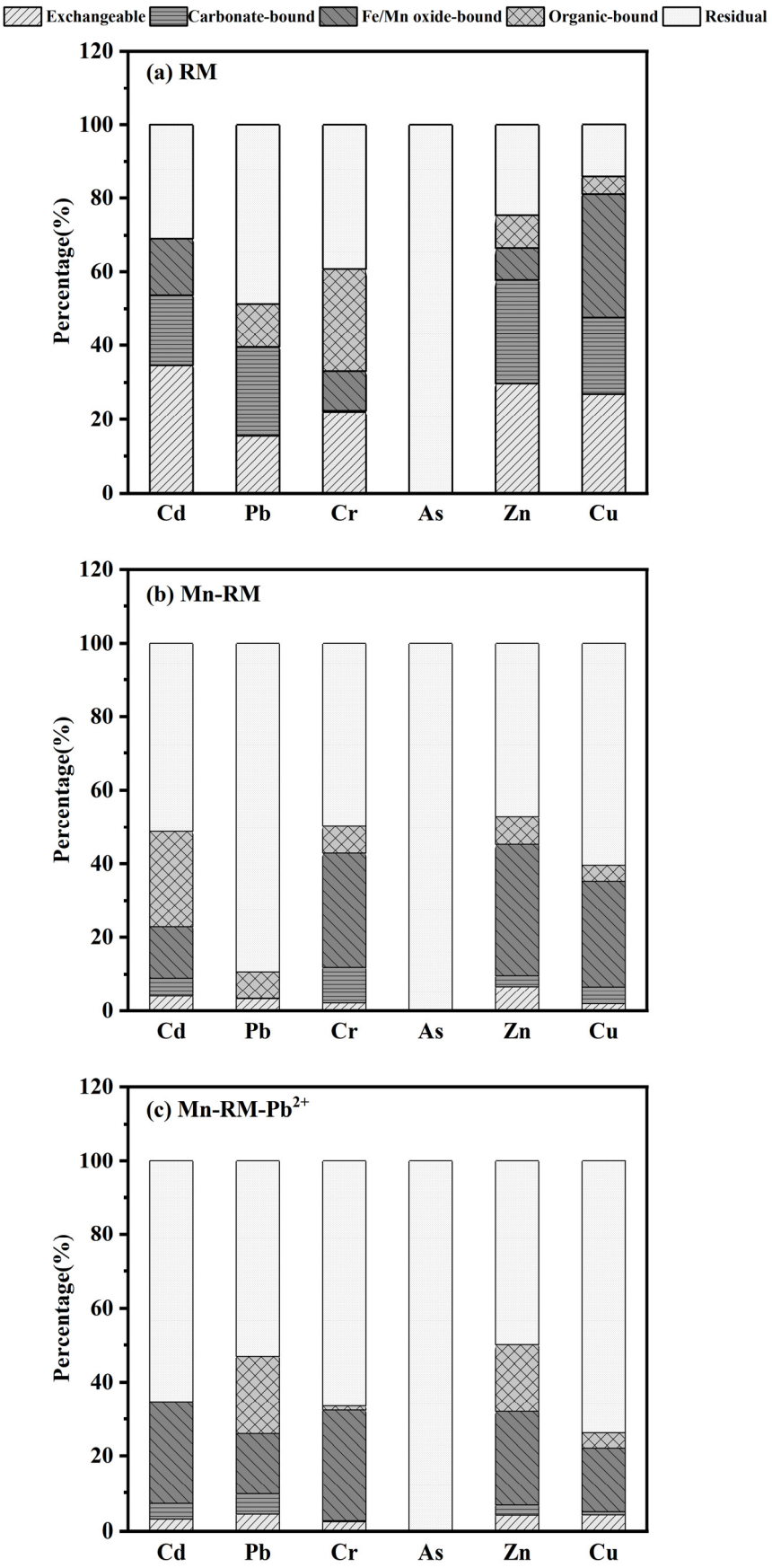

Fig. S6. Fractionation of heavy metals in (a) RM, (b) Mn-RM, and (c) Mn-RM-Pb^{2+}.

References

1. Wang, Z.; Su, J.; Hu, X.; Ali, A.; Wu, Z. Isolation of Biosynthetic Crystals by Microbially Induced Calcium Carbonate Precipitation and Their Utilization for Fluoride Removal from Groundwater. *J. Hazard. Mater.* **2021**, *406*, 124748.
2. Jalil, A.A.; Triwahyono, S.; Yaakob, M.R.; Azmi, Z.Z.A.; Sapawe, N.; Kamarudin, N.H.N.; Setiabudi, H.D.; Jaafar, N.F.; Sidik, S.M.; Adam, S.H.; et al. Utilization of Bivalve Shell-Treated Zea Mays L.(Maize) Husk Leaf as a Low-Cost Biosorbent for Enhanced Adsorption of Malachite Green. *Bioresour. Technol.* **2012**, *120*, 218–224.
3. Xiong, Y.; Zhu, F.; Zhao, L.; Jiang, H.; Zhang, Z. Heavy Metal Speciation in Various Types of Fly Ash from Municipal Solid Waste Incinerator. *J. Mater. Cycles Waste Manag.* **2014**, *16*, 608–615.
4. Izquierdo, M.; Querol, X. Leaching Behaviour of Elements from Coal Combustion Fly Ash: An Overview. *Int. J. Coal Geol.* **2012**, *94*, 54–66.
5. Pan, Y.; Wu, Z.; Zhou, J.; Zhao, J.; Ruan, X.; Liu, J.; Qian, G. Chemical Characteristics and Risk Assessment of Typical Municipal Solid Waste Incineration (MSWI) Fly Ash in China. *J. Hazard. Mater.* **2013**, *261*, 269–276.
6. Li, W.; Sun, Y.; Huang, Y.; Shimaoka, T.; Wang, H.; Wang, Y.; Ma, L.; Zhang, D. Evaluation of Chemical Speciation and Environmental Risk Levels of Heavy Metals during Varied Acid Corrosion Conditions for Raw and Solidified/Stabilized MSWI Fly Ash. *Waste Manag.* **2019**, *87*, 407–416.

7. Luan, J.; Chai, M.; Li, R. Heavy Metal Migration and Potential Environmental Risk Assessment during the Washing Process of MSW Incineration Fly Ash and Molten Slag. *Procedia Environ. Sci.* **2016**, *31*, 351–360.